DOI 10.2478/ama-2025-0089

INFLUENCE OF EXTENSION-SHEARING BENDING-TWISTING AND BENDING-TWSTING COUPLING ON THE BUCKLING BEHAVIOUR OF COMPOSITE PROFILES

Katarzyna FALKOWICZ*

*Faculty, Faculty of Mechanical Engineering, Department of Machine Design and Mechatronics, Lublin University of Technology, Nadbystrzycka 36, 20-618 Lublin, Poland

k.falkowicz@pollub.pl

received 03 November 2025, revised 18 November 2025, accepted 21 November 2025

Abstract: This paper presents a comparative analysis to investigate the effect of laminate stacking sequences with different couplings subjected to axial loading. The objective of this paper is also to demonstrate the effect of the various coupling stiffnesses on the stability behavior of laminated profiles. Five configurations with the same number of layers were selected. Based on Classical Laminate Theory (CLT), the complex effects of coupling that can occur in laminates were assessed. Their influence on the buckling mode and post-buckling behavior of the tested profiles was also assessed. By selecting these standard ply orientations, the study establishes a direct experimental comparison to assess the effect of Bending-Twisting (B-T) coupling and Extension-Shearing Bending-Twisting (E-S, B-T) coupling on buckling behavior of simply supported and axially compressed laminated profiles. The results enable correlation between laminate coupling coefficients and the observed buckling modes obtained from digital image correlation system and axial stiffness of Ω- and Z-profiles.

Key words: stability, couplings, Extension-Shearing (E-S), Bending-Twisting (B-T), buckling

1. INTRODUCTION

Composite materials have attracted considerable attention in recent decades due to their outstanding specific stiffness, strength, and the possibility of tailoring mechanical properties through precise control of the stacking sequence. They are widely utilized in aero-space [1], automotive, marine, civil [2], and biomedical engineering applications [3–6], where lightweight and high-performance structures are required. In laminated fiber-reinforced composites, the arrangement and orientation of individual plies play a decisive role in determining not only the overall stiffness but also the presence of coupling effects between different deformation modes. Such couplings arising from specific combinations of off-axis layers can significantly influence the global and local stability behavior of thin-walled composite components.

The present paper serves as a continuation and complement to the study presented in [7], as well as an introduction to a series of forthcoming papers (which are under review) related to the investigation of the behavior of thin-walled composite structures exhibiting various types of mechanical couplings under axial compression, both at room temperature and under elevated or reduced thermal conditions.

A considerable amount of research has addressed the buckling and post-buckling response of thin-walled composite members with different cross-section shapes [8–10]. Nevertheless, most of these works concentrated mainly on local stability assessment, while the influence of laminate coupling effects was not comprehensively analysed.

In the literature, the most frequently encountered stacking configurations are the standard symmetric angle-ply laminates, i.e. ±45°, 0°, and 90°. Symmetric stacking sequences are widely used in composite laminate design practice, primarily because they ensure that the laminate remains flat and free from distortion after high-temperature curing [11].

Asymmetric laminates, on the other hand, are often associated with configurations that undergo significant deformation after curing at high temperatures or are frequently (and incorrectly) used to describe such behavior [12]. However, as demonstrated in previous studies [13], asymmetric stacking sequences can provide the same thermo-mechanical properties as their symmetric counterparts while belonging to a much broader and largely unexplored design space.

It should be emphasized that numerous investigations dealing with the flexural response of composite laminates, including buckling and post-buckling analyses, commonly employ Bending–Twisting coupled configurations as reference cases. Nevertheless, only a limited number of studies explicitly address the influence of this coupling effect. The omission of Bending–Twisting interactions is often justified by assuming that their impact becomes negligible in laminates composed of many plies. In reality, however, for thin-walled laminates, the buckling performance is significantly affected by such couplings — neglecting them leads to an overestimation of the compressive buckling load, which may result in non-conservative design predictions.

While the Bending–Twisting interaction has been relatively well recognized, considerably less attention has been devoted to another class of mechanical coupling — the Extension–Shearing coupling. In balanced stacking sequences, this effect is typically suppressed by arranging matching pairs of angle-ply layers [14]. Nevertheless, Ch. York in paper [15] presented details of the development of a special class of laminate, possessing Extension-Shearing

Bending-Twisting coupling, necessary for optimized passive-adaptive flexible wing-box structures. However, still many scientific considerations are not experimentally confirmed, which fills the research gap in this topic.

What is more, by intentionally selecting specific configurations, it is possible to activate and examine the impact of both Bending–Twisting and Extension–Shearing couplings under axial compression conditions. The chosen and presented in current paper layouts allows for the evaluation of potential mechanical couplings (e.g., Bending-Twisting, Extension-Shearing) under axial compression conditions of composite profiles including experimental tests.

2. MATERIAL AND METHOD

Laminated composite materials exhibit characteristic responses to mechanical and thermal loading, governed by their intrinsic coupling behavior. Equation (1) describes well- known ABD relation, according to the classical lamination theory [12,16]:

$$\begin{Bmatrix} N \\ M \end{Bmatrix} = \begin{bmatrix} A & B \\ B & D \end{bmatrix} \begin{Bmatrix} \varepsilon \\ \kappa \end{Bmatrix} \tag{1}$$

where: N and M – internal forces and moments; ε and the mid-plane κ – strains and curvatures of the laminate respectively; A,B,D – are the stiffness matrices: extensional [A], coupling [B] and bending [D].

The elements of the stiffness matrices can be calculated from below equations:

$$A_{ij} = \sum_{k=1}^{n} Q'_{ij} (z_k - z_{k-1})$$

$$B_{ij} = \sum_{k=1}^{n} Q'_{ij} (z_k^2 - z_{k-1}^2)/2$$

$$D_{ij} = \sum_{k=1}^{n} Q'_{ij} (z_k^3 - z_{k-1}^3)/3 \tag{2}$$

in which the summations extend over all *n* plies; Q'_{ij} are the transformed reduced stiffnesses (*i*, *j* = 1, 2, 6) and *z* represents the distance of the k^{th} ply from the laminate mid-plane

The behavior of couplings type considered in this study are summarized in Fig.1. In all analyzed configurations, the coupling between in-plane (membrane) and out-of-plane (bending or flexural) responses—and thus thermal warping distortions—is eliminated, as B_{ij} = 0 (or B_{16}=B_{26}=0) in Eq. (1). Nevertheless, coupling between in-plane shear and extension may occur when A_{16} = A_{26} ≠ 0, and/or bending–twisting coupling appears when D_{16} = D_{26} ≠ 0.

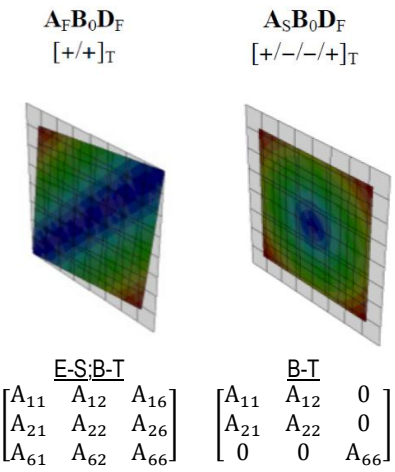

B=0
$\begin{bmatrix} D_{11} & D_{12} & D_{16} \\ D_{21} & D_{22} & D_{26} \\ D_{61} & D_{62} & D_{66} \end{bmatrix}$
a)

B=0
$\begin{bmatrix} D_{11} & D_{12} & D_{16} \\ D_{21} & D_{22} & D_{26} \\ D_{61} & D_{62} & D_{66} \end{bmatrix}$
b)

Fig. 1. Coupling responses, in relation to the cases under consideration, for due to free thermal contraction, for laminates with: a) Shearing -Extension and Bending-Twisting (E-S; B-T laminate), b) Bending-Twisting coupling (B-T laminate) [17]

Figure 2 present a of comprehensive set of deformation hypotheses from Classical Laminate Theory (CLT) leading to the force-strain-curvature and moment-strain-curvature relations, where the A_{ij}, B_{ij} and D_{ij} are labeled. There A_{16} and A_{26} represent shear-extension coupling, B_{ij} represent coupling between bending and extension, D_{16} and D_{26} represent bending-twisting coupling.

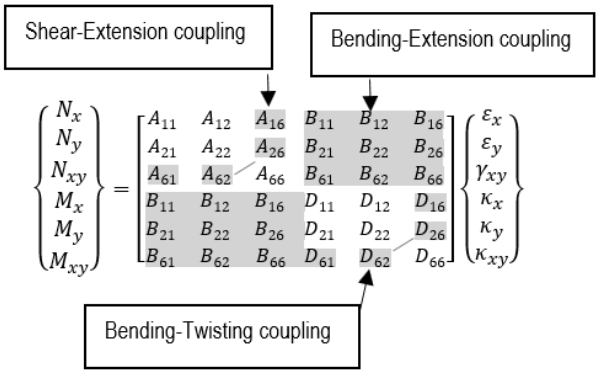

Fig. 2. Physical significance of stiffness terms in force and moment resultants

To investigate the influence of laminate coupling on the compressive stability of thin-walled composite Ω- and Z-profiles, a series of quasi-symmetric laminates with graded fibre orientations was manufactured (Fig.8) and tested. Five nominally symmetric stacking sequences were designed: [0/30/45/60/90]s, [90/60/45/30/0]s, [90/0/0/45/−45]s, [45/−45/0/0/90]s and [0/0/45/−45/90]s (Tab. 1).

Tab. 1. Considered layer layouts with type of mechanical couplings

No.	Sequences	Subscript notation ESDU (1994) [14]	Coupling type
L1	$[0/30/45/60/90]_s$	$A_FB_0D_F$	S-E, T-B
L2	$[90/60/45/30/0]_s$	$A_FB_0D_F$	S-E, T-B
L3	$[90/0/0/45/-45]_s$	$A_SB_0D_F$	T-B
L4	$[45/-45/0/0/90]_s$	$A_SB_0D_F$	T-B
L5	$[0/0/45/-45/90]_s$	$A_SB_0D_F$	T-B

Although these laminates are denoted with the symmetry subscript "s", their angular gradation or asymmetrical ply combinations introduce measurable coupling effects that deviate from ideal symmetry. We can observe this phenomenon when we will made calculations of the ABD matrix components (Eq. 3-7). All calculations

were performed using the own algorithm based on the standard equations. Indeed, most fully uncoupled laminates are non-symmetric by nature. Calculations of ABD matrix were performed for a carbon-fibre epoxy material with Young's moduli E_1=118.32 GPa, E_2=8.34 GPa, shear modulus G_{12}=4.6 GPa and Poisson's ratio v_{12}=0.31, thickness t=0.1mm(10x0.1=1mm) [18,19].

Laminate 1

The Eq. (3) present the ABD matrix for Laminate 1, with axis aligned properties, represents S-E, T-B coupling. By inspection, $A_{11} = A_{22}$, and by calculation, $A_{66} = (A_{11} - A_{12})/2 = 17.59$ N/mm, revealing that the laminate possesses in-plane isotropic properties.

$$\begin{Bmatrix} N_x \\ N_y \\ N_{xy} \\ M_x \\ M_y \\ M_{xy} \end{Bmatrix} = \begin{bmatrix} 50.772 & 15.593 & 15.126 & 0 & 0 & 0 \\ 15.593 & 50.772 & 15.126 & 0 & 0 & 0 \\ 15.126 & 15.126 & 17.590 & 0 & 0 & 0 \\ 0 & 0 & 0 & 7.181 & 1.118 & 1.279 \\ 0 & 0 & 0 & 1.118 & 1.645 & 0.829 \\ 0 & 0 & 0 & 1.279 & 0.829 & 1.284 \end{bmatrix} \begin{Bmatrix} \varepsilon_x \\ \varepsilon_y \\ \gamma_{xy} \\ \kappa_x \\ \kappa_y \\ \kappa_{xy} \end{Bmatrix} \tag{3}$$

The laminate [0/30/45/60/90]s exhibits a monotonic fibre angle progression producing non-zero D_{16} and D_{26} terms, while maintaining approximate bending symmetry.

The [0/30/45/60/90]s laminate represents a graded-angle quasi-symmetric configuration designed to introduce controlled coupling through a gradual fibre orientation transition across the thickness.

Such graded laminates are commonly employed in aeroelastic tailoring, where fibre orientation gradients enable directional stiffness tuning and load redistribution without compromising bending symmetry.

The configuration was chosen to explore the influence of progressive angular transitions on the compressive stability of Z- and Ω-section profiles.

Laminate 2

The Eq. (4) present the ABD matrix for Laminate 2, with axis aligned properties, represents S-E, T-B coupling. By inspection, $A_{11} = A_{22}$, and by calculation, $A_{66} = (A_{11} - A_{12})/2 = 17.59$ N/mm, revealing that the laminate possesses in-plane isotropic properties.

$$\begin{Bmatrix} N_x \\ N_y \\ N_{xy} \\ M_x \\ M_y \\ M_{xy} \end{Bmatrix} = \begin{bmatrix} 50.769 & 15.594 & 15.126 & 0 & 0 & 0 \\ 5.594 & 50.769 & 15.126 & 0 & 0 & 0 \\ 15.126 & 15.126 & 17.587 & 0 & 0 & 0 \\ 0 & 0 & 0 & 1.644 & 1.118 & 0.829 \\ 0 & 0 & 0 & 1.118 & 7.181 & 1.279 \\ 0 & 0 & 0 & 0.829 & 1.279 & 1.284 \end{bmatrix} \begin{Bmatrix} \varepsilon_x \\ \varepsilon_y \\ \gamma_{xy} \\ \kappa_x \\ \kappa_y \\ \kappa_{xy} \end{Bmatrix} \tag{4}$$

The [90/60/45/30/0]s laminate is the reversed counterpart of the graded configuration [0/30/45/60/90]s, arranged in an opposite angular order.

This design allows assessment of how the direction of fibre angle progression affects laminate coupling and the resulting asymmetry in bending and twisting responses.

The reverse orientation swaps the values of the coupling coefficients D_{16} and D_{26}, and D_{11} and D_{22}.

Laminate 3

The Eq. (5) present the ABD matrix for Laminate 3, with axis aligned properties, represents T-B coupling.

$$\begin{Bmatrix} N_x \\ N_y \\ N_{xy} \\ M_x \\ M_y \\ M_{xy} \end{Bmatrix} = \begin{bmatrix} 64.440 & 12.996 & 0 & 0 & 0 & 0 \\ 12.996 & 42.294 & 0 & 0 & 0 & 0 \\ 0 & 0 & 14.989 & 0 & 0 & 0 \\ 0 & 0 & 0 & 4.990 & 0.355 & 0.111 \\ 0 & 0 & 0 & 0.355 & 5.359 & 0.111 \\ 0 & 0 & 0 & 0.111 & 0.111 & 0.522 \end{bmatrix} \begin{Bmatrix} \varepsilon_x \\ \varepsilon_y \\ \gamma_{xy} \\ \kappa_x \\ \kappa_y \\ \kappa_{xy} \end{Bmatrix} \tag{5}$$

The [90/0/0/45/−45]s laminate serves as a quasi-isotropic baseline configuration.

This sequence minimizes coupling effects and serves as a control case for evaluating the influence of angular asymmetry in other laminates.

Laminate 4

The Eq. (6) present the ABD matrix for Laminate 5, with axis aligned properties, represents T-B coupling.

$$\begin{Bmatrix} N_x \\ N_y \\ N_{xy} \\ M_x \\ M_y \\ M_{xy} \end{Bmatrix} = \begin{bmatrix} 64.440 & 12.996 & 0 & 0 & 0 & 0 \\ 12.996 & 42.294 & 0 & 0 & 0 & 0 \\ 0 & 0 & 14.989 & 0 & 0 & 0 \\ 0 & 0 & 0 & 4.539 & 1.914 & 0.443 \\ 0 & 0 & 0 & 1.914 & 2.693 & 0.443 \\ 0 & 0 & 0 & 0.443 & 0.443 & 2.081 \end{bmatrix} \begin{Bmatrix} \varepsilon_x \\ \varepsilon_y \\ \gamma_{xy} \\ \kappa_x \\ \kappa_y \\ \kappa_{xy} \end{Bmatrix} \tag{6}$$

The stacking sequence [45/−45/0/0/90]s was selected as a quasi-symmetric laminate containing a double 0° sublaminate.

Although its structure superficially resembles a pseudo double–double configuration, it does not satisfy the formal definition proposed by [20] in which a double–double laminate consists exclusively of two distinct non-opposite angles arranged in balanced $\pm\theta_1$ and $\pm\theta_2$ pairs.

In contrast, the present [45/−45/0/0/90]s laminate includes both ±45° off-axis plies and a double 0° core, resulting in full geometric symmetry ([B] = 0) while maintaining enhanced axial stiffness and partial in-plane balance.

Such configurations are commonly referred to in literature as quasi-symmetric laminates with double [21,22] and are often used to replicate the mechanical behaviour of double–double systems without introducing additional manufacturing complexity.

The inclusion of two consecutive 0° plies was intended to reinforce the longitudinal stiffness of the profile, providing improved compressive strength while preserving the symmetric response under axial loading.

Laminate 5

The Eq. (7) present the ABD matrix for Laminate 6, with axis aligned properties, represents T-B coupling.

$$\begin{Bmatrix} N_x \\ N_y \\ N_{xy} \\ M_x \\ M_y \\ M_{xy} \end{Bmatrix} = \begin{bmatrix} 64.443 & 12.995 & 0 & 0 & 0 & 0 \\ 12.995 & 42.297 & 0 & 0 & 0 & 0 \\ 0 & 0 & 14.992 & 0 & 0 & 0 \\ 0 & 0 & 0 & 8.443 & 0.667 & 0.221 \\ 0 & 0 & 0 & 0.667 & 1.283 & 0.221 \\ 0 & 0 & 0 & 0.221 & 0.221 & 0.834 \end{bmatrix} \begin{Bmatrix} \varepsilon_x \\ \varepsilon_y \\ \gamma_{xy} \\ \kappa_x \\ \kappa_y \\ \kappa_{xy} \end{Bmatrix} \quad (7)$$

The [0/0/45/−45/90]s laminate serves as a quasi-isotropic baseline configuration.

This sequence minimizes coupling effects and serves as a control case for evaluating the influence of angular asymmetry in other laminates.

According to the results presented in the case study, changing the lamina orientations while maintaining equal angles between the adjacent plies, means to obtain different [B] and [D] matrices, but same [A] matrix.

3. DISCUSSION

Nemeth's research demonstrated that the interaction between bending and twisting deformations, described by the D_{16} and D_{26} terms, plays a crucial role in determining the buckling response of composite laminates [23]. An increase in bending–twisting anisotropy, especially for laminates exhibiting higher D_{26} values, leads to the appearance of inclined or spiral-shaped buckling modes. The corresponding magnitudes of the D_{16} and D_{26} coefficients are illustrated in Figure 3, while Figure 4 additionally presents the A_{16} and A_{26} terms, which are associated with in-plane shear–extension coupling. To evaluate the overall anisotropic behaviour and its effect on structural stability, Nemeth introduced three flexural anisotropy parameters: β, δ and γ, (Eq. 8-10) derived from the D_{16} and D_{26} coupling components. β and γ describe the global bending anisotropy (the ratio of stiffnesses in the principal directions), δ describes the bending–twisting coupling intensity. The computed values of these parameters for the laminates examined in this study are provided in Figures 5-7. According to Nemeth, an increase in the δ parameter corresponds to a stronger degree of coupling, which is directly linked to departures from classical buckling shapes and the emergence of more complex deformation modes.

$$\beta = \frac{D_{12}+2*D_{66}}{\sqrt[2]{D_{11}*D_{22}}} \quad (8)$$

$$\gamma = \frac{D_{16}}{\sqrt[4]{D_{11}^3*D_{22}}} \quad (9)$$

$$\delta = \frac{D_{26}}{\sqrt[4]{D_{22}^3*D_{11}}} \quad (10)$$

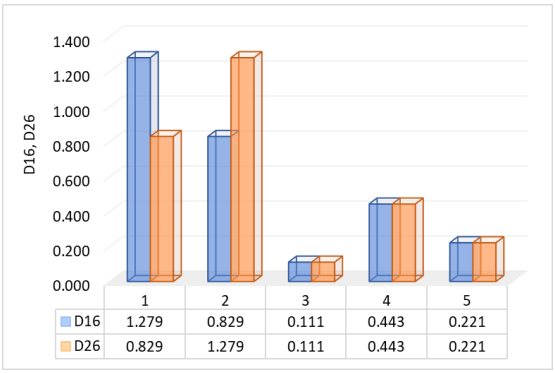

Fig. 3. The coefficients D_{16} and D_{26} value for all considered configurations

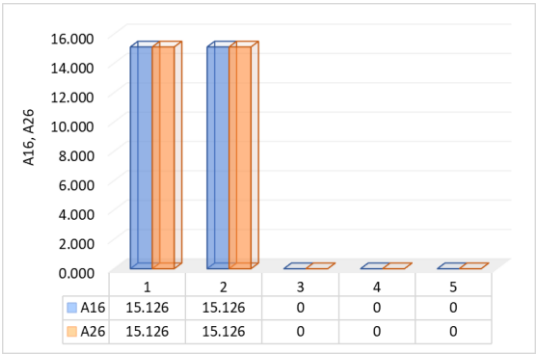

Fig. 4. Effects of mechanical couplings on the coefficients A_{16} and A_{26}

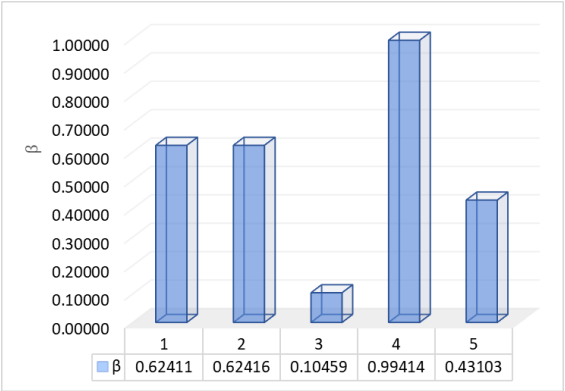

Fig. 5. Nondimensional flexural anisotropy parameter β value for all considered configurations

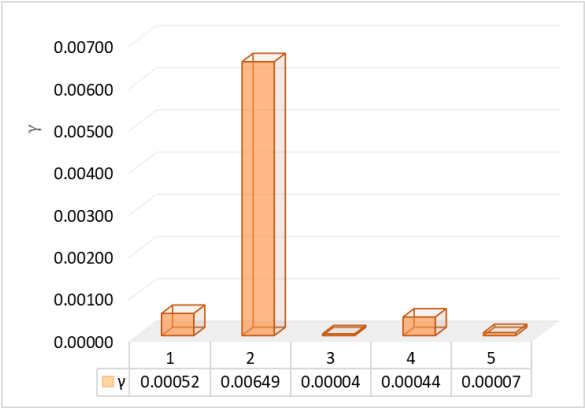

Fig. 6. Nondimensional flexural anisotropy parameter γ value for all considered configurations

DOI 10.2478/ama-2025-0089

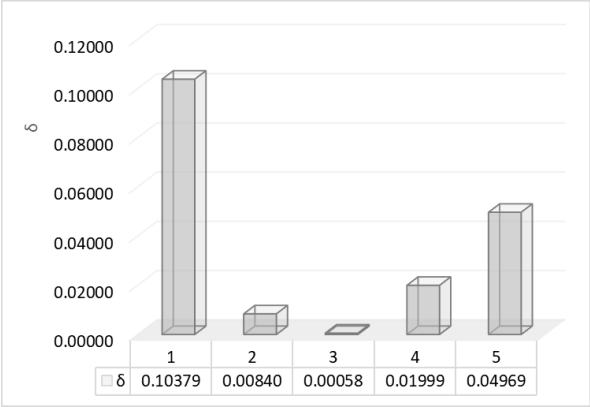

Fig. 7. Value of nondimensional flexural anisotropy parameter δ for all considered configurations

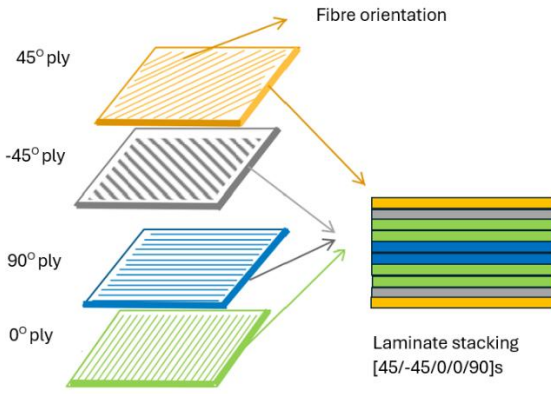

c)

Fig. 8. Manufacture samples: a) Ω-section profile, b) Z-section profile, c) the example of cross-section of chosen configuration

To investigate the influence of the selected stacking sequences, which include identified mechanical couplings, on the behaviour of typical composite profiles, specimens with omega-shaped and Z-shaped cross-sections were manufactured. Figure 8 presents the fabricated profiles together with their corresponding cross-sectional dimensions. The total profile height was H = 150 mm. The experimental setup is shown in Figure 9. All tests were conducted using a universal testing machine (MTS 809) integrated with the ARAMIS digital image correlation (DIC) system. More information about performed experimental test presented in [7]. Figures 10 and 11 illustrate the buckling modes observed for the tested specimens, accompanied by the corresponding deformation maps obtained from the ARAMIS system. In table 2 values for critical forces were compiled. The graphs shown in Figures 12 and 13 present the post-buckling equilibrium paths, recorded directly by the testing machine during the experiments.

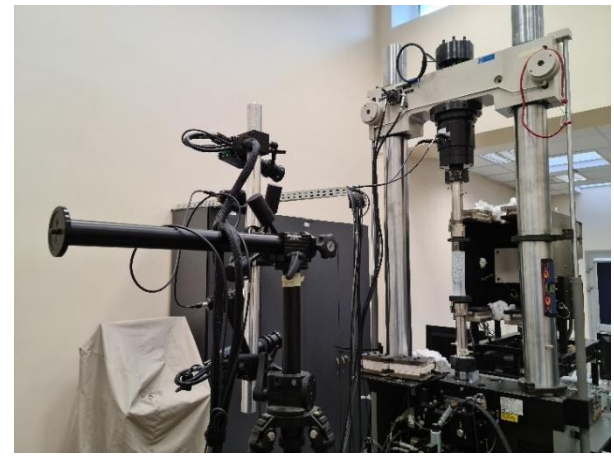

Fig. 9. Experimental test stand

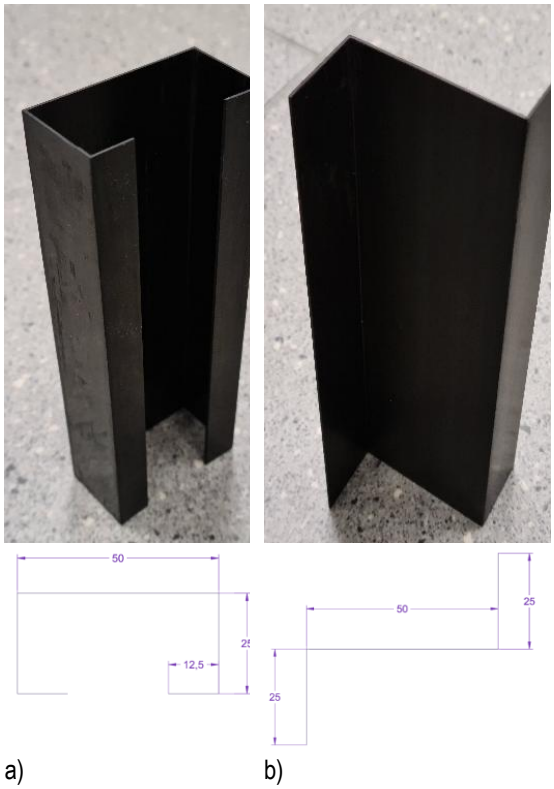

a) b)

a) b)

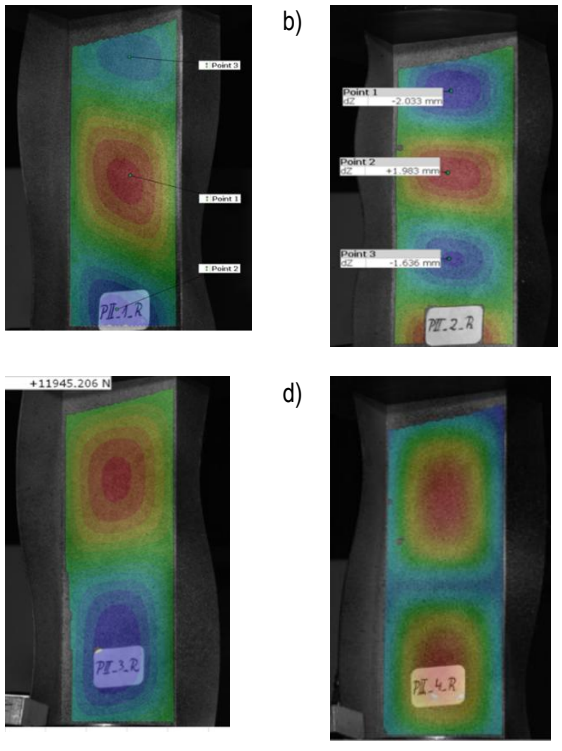

c) d)

e)

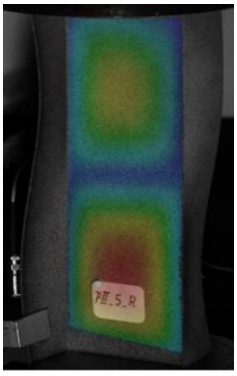

Fig. 10. Experimental buckling mode (with DIC maps) for Z-cross section profiles: a) L1, b) L2, c) L3, d) L4, e) L5

a) b)

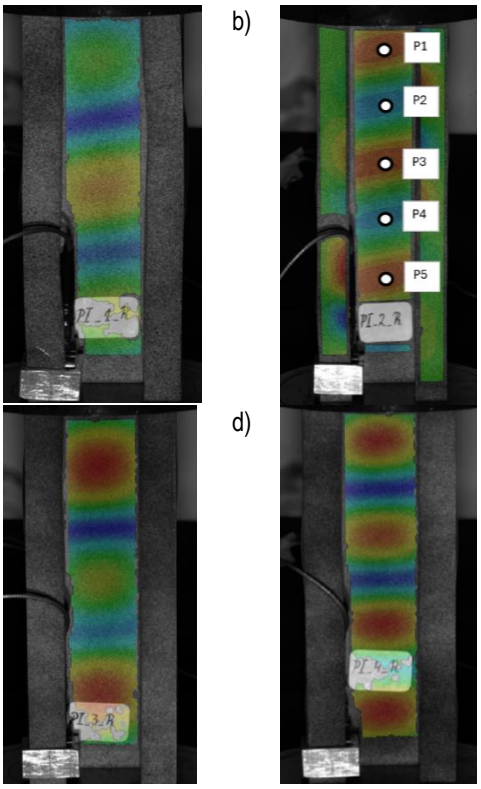

c) d)

e)

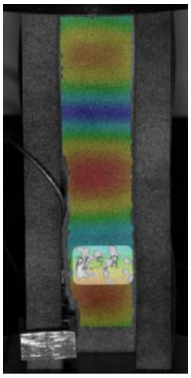

Fig. 11. Experimental buckling mode (with DIC maps) for omega cross section profiles: a) L1, b) L2, c) L3, d) L4, e) L5

According to Nemeth, an increase in the δ parameter corresponds to a greater degree of coupling, which is directly related to the departure from classical buckling shapes and the emergence of more complex deformation modes. According to Nemeth The δ parameter governs the rotation of the principal curvature axes and determines whether the plate buckles in a symmetric or inclined mode. However, looking at the obtained buckling modes and the increase in the δ and γ parameters, the most complex buckling mode is assumed by Laminate 1 and 2. Nevertheless, for L1 parameters δ is the highest - the greatest bending-twisting coupling, which perfectly explains the oblique and spiral buckling modes (Fig. 10 a)). For L2 the coupling effect a little disappears, resulting in a more symmetrical mode (in Z-cross section). It is worth noting here that the L2 system is a mirror layouts of the L1 layouts and this change is clearly visible in Fig. 6 and Fig. 7 when changing the γ and δ parameters. For L3 no coupling, pure buckling mode and for L4, L5 slight coupling, i.e. quasi-symmetric systems.

Tab. 2. Buckling load value

No. laminate	Bucklin load [N] for Ω-section	Bucklin load [N] for Z-section
L1	8299.5	3301.6
L2	7832.5	3386.6
L3	10217	3352.3
L4	11953	5326.2
L5	8020.2	3386.0

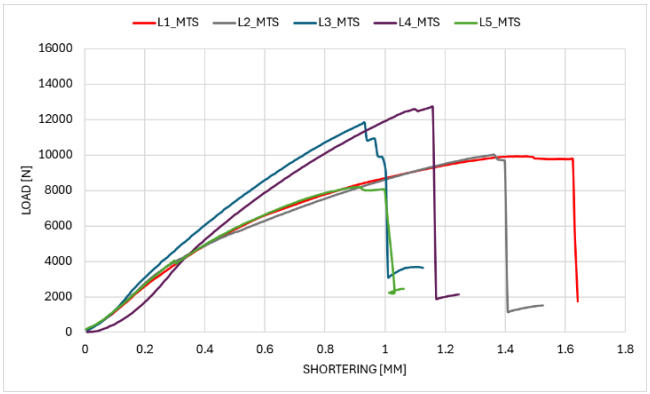

Fig. 12. Experimental postbuckling equilibrium paths of Z-section profile for all cases

The introduction of combined couplings did not increase the initial buckling load – in fact, the coupled layups often buckled at slightly lower loads than a stiff, uncoupled design. For example, the Ω-profile with combined coupling (L1) had ~20% lower buckling load than a quasi-isotropic baseline laminate (L3), illustrating the trade-off for coupling-induced anisotropy. However, the key benefit of combining B–T and E–S couplings was observed in the post-buckling regime. These laminates showed the greatest post-buckling rigidity, meaning that after initial buckling they carried additional load with only small deflection increases. In practical terms, the coupled profiles exhibited a more stable post-buckling response – instead of a dramatic drop in load capacity after buckling, the load–deflection curve was nearly flat or rising, indicating the structure can sustain higher loads beyond buckling. The combined coupling scenario suggests a deliberate design strategy for thin-walled composites: one can allow an early, benign buckling at a lower load in exchange for a higher reserve strength afterward.

Overall, the laminate characterized by combined bending–twisting and extension–shearing couplings (D_{16}, D_{26}, A_{16}, $A_{26} \neq 0$) exhibited the greatest post-buckling rigidity, making it the most significant configuration among the analysed cases.

DOI 10.2478/ama-2025-0089

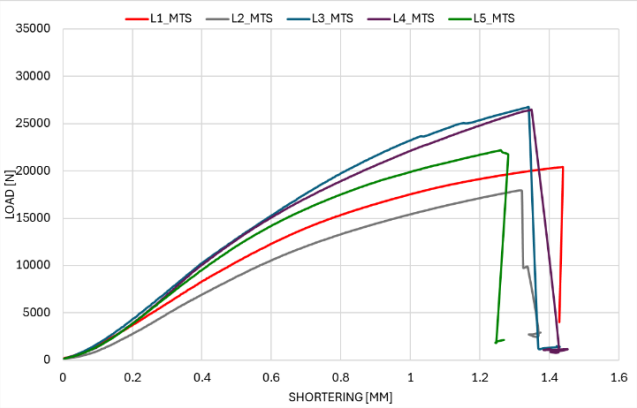

Fig. 13. Experimental postbuckling equilibrium paths of Ω-section profile for all cases

4. SUMMARY AND SCIENTIFIC SIGNIFICANCE

By selecting these particular layups, the study establishes a direct experimental comparison between Bending-Twisting coupling and Extension-Shearing Bending-Twisting coupling on buckling behavior of simply supported compressed laminated profiles. The results enable correlation between laminate coupling coefficients (A_{16}, A_{26}, D_{16}, D_{26}) and the observed buckling modes and axial stiffness of Ω- and Z-profiles.

According to the results presented in the case study, changing the lamina orientations while maintaining equal angles between the adjacent plies, means to obtain different [D] matrices, but same [A] matrix. Moreover, the stacking sequence has a great influence on strain and stress distributions, as well as on buckling mode and critical load value.

Bending–Twisting (B–T) as well as Bending–Twisting (B–T) and Extension – Shearing (E-S) combination of coupling was found to have a significant impact on the buckling behaviour of the analysed laminates. The presence of this coupling favoured deviations from classical buckling modes – for larger values of D_{16} and D_{26}, unusual, oblique, or torsional buckling modes appeared. In the case of simultaneous occurrence of both couplings (B–T and E–S), a significant improvement in the stability characteristics of the structure was observed- higher reserve strength afterward.

The obtained results have significant implications for the design of thin-walled composite structures. Neglecting mechanical couplings (especially the bending-twisting effect) in stability analyses can lead to a non-conservative overestimation of the critical load. From a design perspective, it is therefore advisable to consider the influence of B–T couplings (and, if necessary, E–S couplings) when selecting the laminate ply configuration. Furthermore, conscious gradation of fiber orientation allows for the introduction of controlled couplings, which – as has been shown – can increase the stiffness and load-bearing capacity of a structure after buckling without significantly reducing the critical load. The skillful use of mechanical couplings therefore offers a promising avenue for optimizing structures for stability and material efficiency.

The presented results demonstrate that bending–twisting and extension–shear couplings can be deliberately exploited in the design of thin-walled composite structures to tailor their stability response, what can have a bearing under variable thermal conditions. Such couplings offer a promising passive mechanism for load redistribution, post-buckling control, and enhanced load-carrying capacity in advanced lightweight engineering applications.

This study builds upon the work of Ch. York [15,24,25]by providing experimental verification of selected laminate configurations. More importantly, it serves as an introduction to further investigations into the influence of specific mechanical couplings on the buckling and post-buckling behavior of composite profiles, as well as their stability performance under varying thermal conditions.

Furthermore, the results demonstrate that even seemingly symmetric configurations may exhibit coupling effects, since most fully uncoupled laminates are inherently non-symmetric. These residual couplings can still influence the buckling response to varying degrees. Nevertheless, more complex coupling effects are typically associated with intentionally non-symmetric layups, some of which were partially tested during the Bekker Fellowship and will be discussed in future publications.

REFERENCES

1. Kopecki T, Bakunowicz J, Lis T. Post-critical deformation states of composite thin-walled aircraft load-bearing structures. jtam. 2016;195.
2. Chróścielewski J, Miśkiewicz M, Pyrzowski Ł, Sobczyk B, Wilde K. A novel sandwich footbridge - Practical application of laminated composites in bridge design and in situ measurements of static response. Composites Part B: Engineering. 2017;126:153–61.
3. Karpiński R, Szabelski J, Krakowski P, Jonak J, Falkowicz K, Jojczuk M, et al. Effect of various admixtures on selected mechanical properties of medium viscosity bone cements: Part 3 – Glassy carbon. Composite Structures. 2024;343:118307.
4. Karpiński R, Szabelski J, Krakowski P, Jonak J, Falkowicz K, Jojczuk M, et al. Effect of various admixtures on selected mechanical properties of medium viscosity bone cements: Part 2 – Hydroxyapatite. Composite Structures. 2024;343:118308.
5. Karpiński R, Szabelski J, Krakowski P, Jonak J, Falkowicz K, Jojczuk M, et al. Effect of various admixtures on selected mechanical properties of medium viscosity bone cements: Part 1 – α/β tricalcium phosphate (TCP). Composite Structures. 2024;343:118306.
6. Wysmulski P, Debski H, Falkowicz K. Sensitivity of Compressed Composite Channel Columns to Eccentric Loading. Materials. 2022;15:6938.
7. Falkowicz K, Kuciej M, Świech Ł. Temperature Effect on Buckling Properties of Thin-Walled Composite Profile Subjected to Axial Compression. Adv. Sci. Technol. Res. J. 2024;18:305–13.
8. Falkowicz K. Numerical Buckling Analysis of Thin-Walled Channel-Section Composite Profiles Weakened by Cut-Outs. Adv. Sci. Technol. Res. J. 2022;16:88–96.
9. Banat D, Mania RJ, Degenhardt R. Stress state failure analysis of thin-walled GLARE composite members subjected to axial loading in the post-buckling range. Composite Structures. 2022;289:115468.
10. Kubiak T, Samborski S, Teter A. Experimental investigation of failure process in compressed channel-section GFRP laminate columns assisted with the acoustic emission method. Composite Structures. 2015;133:921–9.
11. Niu C, redaktor. Composite airframe structures: practical design information and data. 3rd ed. Hong Kong: Conmilit Press; 2010.
12. Jones RM. Mechanics of Composite Materials [Internet]. 2. wyd. CRC Press; 2018.
Available from: https://www.taylorfrancis.com/books/9781498711067
13. York CB. Tapered hygro-thermally curvature-stable laminates with non-standard ply orientations. Composites Part A: Applied Science and Manufacturing. 2013;44:140–8.
14. ESDU. Stiffnesses of laminated plates. Engineering sciences data unit. Item no. 94003; 1994.
15. York CB, De Almeida SFM. On Extension-Shearing Bending-Twisting coupled laminates. Composite Structures. 2017;164:10–22.

16. H. Altenbach, J.W. Altenbach, W. Kissing. Mechanics of composite structural elements. Berlin Heilderberg: Springer; 2013.
17. York C. Unified approach to the characterization of coupled composite laminates: Hygro-thermally curvature-stable configurations. International Journal of Structural Integrity. 2011;2:406–36.
18. Falkowicz K. Material properties of CFRP composite [Internet]. 2025. Available from: https://repod.icm.edu.pl/citation?persistentId=doi:10.18150/YKBDJQ
19. Falkowicz K. Determined material properties within the framework of the NCN project (OPUS) No. 2022/47/B/ST8/00600 [Internet]. 2025. Available from: https://zenodo.org/doi/10.5281/zenodo.15037571
20. Tsai SW. Double–Double: New Family of Composite Laminates. AIAA Journal. 2021;59:4293–305.
21. York CB. Unified Approach to the Characterization of Coupled Composite Laminates: Benchmark Configurations and Special Cases. J. Aerosp. Eng. 2010;23:219–42.
22. York C. Stacking Sequences for Extensionally Isotropic, Fully Isotropic and Quasi-Homogeneous Orthotropic Laminates [Internet]. W: 49th AIAA/ASME/ASCE/AHS/ASC Structures, Structural Dynamics, and Materials Conference
 16th AIAA/ASME/AHS Adaptive Structures Conference
 10t. Schaumburg, IL: American Institute of Aeronautics and Astronautics; 2008. Available from: http://arc.aiaa.org/doi/abs/10.2514/6.2008-1940.
23. Nemeth MP. Importance of anisotropy on buckling of compression-loaded symmetriccomposite plates. AIAA Journal 1986;24:1831–5.
24. York CB. On Bending-Twisting coupled laminates. Composite Structures. 2017;160:887–900.
25. York CB, De Almeida SFM. Effect of bending-twisting coupling on the compression and shear buckling strength of infinitely long plates. Composite Structures. 2018;184:18–29.

This research was funded in part by the National Science Centre Poland under the project UMO-2022/47/B/ST8/00600. For the purpose of Open Access, the author has applied a CC-BY public copyright licence to any Author Accepted Manuscript (AAM) version arising from this submission.

The author gratefully acknowledges the valuable guidance and support of prof. Ch. B. York from the Singapore Institute of Technology during the Bekker Fellowship stay. The knowledge gained during the fellowship under project No. BPN/BEK/2024/1/00229/U/00001, financed by the Polish National Agency for Academic Exchange, was utilized in this research.

Katarzyna Falkowicz: https://orcid.org/0000-0002-3007-1462